JACC Vol. 17, No. 3
March 1, 1991:821–7

Natural Evolution of Cardiac Function, Cardiac Pathology and Antimyosin Scan in a Murine Myocarditis Model

CHIHARU KISHIMOTO, MD, PhD, GUO-LONG HUNG, MD, MASATOSHI ISHIBASHI, MD, PhD,* BAN AN KHAW, PhD,* GERALD M. KOLODNY, MD, WALTER H. ABELMANN, MD, FACC, TSUNEHIRO YASUDA, MD*

Boston, Massachusetts

Serial technetium-99m radionuclide ventriculograms, indium-111 antimyosin antibody scans and tissue biodistribution studies were performed in C_3H/He mice with experimentally induced viral encephalomyocarditis and the results were compared with pathologic assessments of myocardial necrosis. Postinfection ejection fraction decreased on days 10 (20.7 ± 5.5%, n = 6), 20 (18.6 ± 15.2%, n = 5), 30 (18.5 ± 7.7%, n = 5) and 150 (30.0 ± 18.7, n = 6) ($p < 0.001$) in comparison with that in uninfected control mice (63.3 ± 3.1%, n = 6).

In the same group of animals, indium-111 antimyosin antibody scans showed intense positive myocardial accumulation on day 10 (in six of six mice) and only slight accumulation on day 20 (in one of five mice). In the chronic stage, two of five mice on day 30 and two of six mice on day 150 still showed positive uptake. The antimyosin scan myocardium to lung uptake ratio (expressed as mean count density [mean counts/pixel of the region] ratio) increased greatly on day 10 ($p < 0.001$ versus values in uninfected control mice) but not subsequently.

Biodistribution studies of the indium-111 antimyosin antibody showed that the heart to blood count ratio was significantly higher on day 10 ($p < 0.001$ versus values in control mice) but not on days 20, 30 and 150. Pathologic examination showed active and ongoing severe myocardial necrosis with dilated ventricles on day 10. On day 20, there was less active necrosis and healing had appeared to begin. On days 30 and 150, myocardial fibrosis increased.

This study reveals a depression in cardiac function in the acute stage of myocarditis that correlates with severe myocardial necrosis and intense uptake of radiolabeled antimyosin. Severe left ventricular dysfunction appeared within 10 days of infection with the encephalomyocarditis virus and continued until day 30. After 5 months, left ventricular function improved in mice that had survived.

(J Am Coll Cardiol 1991;17:821–7)

With the increasing use of myocardial biopsy, myocarditis is becoming more widely diagnosed (1,2). Subacute and chronic forms of myocarditis have been recognized as important causes of morbidity and mortality, and myocarditis is now accepted as one of the important primary as well as contributory causes of chronic dilated cardiomyopathy (2–4). In most cases, the diagnosis of myocarditis is based on clinical findings. However, a definitive diagnosis requires positive evidence of myocarditis by histologic examination. The sensitivity of right ventricular endomyocardial biopsy is not satisfactory; in view of the focal nature of myocarditis, endomyocardial biopsy may lack sensitivity because it may fail to sample a sufficient number of myocardial sites (1). Recently, indium-111 monoclonal antimyosin antibody imaging has been used to clinically diagnose myocarditis (5,6). Because of our interest in viruses as a cause of cardiomyopathy, we (7,8) previously studied cardiac lesions produced by the encephalomyocarditis virus in C_3H/He mice.

In the present study, we attempt to answer three questions: 1) Does acute viral myocarditis cause a decrease in left ventricular ejection fraction? If it does, what are the characteristics of the time course of this decrease? Do the animals deteriorate slowly or rapidly, or do they recover 5 months after the infection? 2) Does the time course of the effect of the disease on left ventricular ejection fraction correlate with pathologic characteristics of myocarditis? 3) Can a noninvasive diagnosis of the presence of myocardial cell necrosis by indium-111 antimyosin antibody scan be used to detect and monitor the natural course of viral myocarditis?

To answer these questions, biodistribution studies were performed to verify results from antimyosin scanning, which were in turn confirmed by pathologic examination.

From the Charles A. Dana Research Institute and the Harvard-Thorndike Laboratory of Beth Israel Hospital and the Cardiovascular and Nuclear Medicine Divisions, Beth Israel Hospital and Harvard Medical School and *Division of Nuclear Medicine and Cardiac Unit, Massachusetts General Hospital and Harvard Medical School, Boston, Massachusetts. This study was supported in part by Ischemia SCOR Grant HL-26205 from the National Heart, Lung, and Blood Institute, Bethesda, Maryland.

Manuscript received July 3, 1990; revised manuscript received September 5, 1990, accepted September 21, 1990.

Address for reprints: Tsunehiro Yasuda, MD, Tilton 2, Massachusetts General Hospital, Boston, Massachusetts 02114.

0735-1097/91/$3.50

Methods

Virus and cells. Encephalomyocarditis virus stock was prepared in cultures of VERO (African green monkey kidney) cells in Eagle's minimum essential medium, and the suspensions were centrifuged after the development of a cytopathic effect. The titer of the virus stock, measured by the formation of plaque on VERO cell monolayers, was $>10^9$ plaque-forming units/0.1 ml. Virus fluid was stored at −70°C until use. Cells were suspended at a concentration of 1×10^6 in Eagle's minimum essential medium with 3% fetal calf serum and 100 μg/ml of penicillin and streptomycin in six well plastic plates and were allowed to grow for 2 days at 37°C in 5% carbon dioxide (CO_2). In plaque assays, volumes (0.1 ml) of decimal dilutions of virus suspended in Eagle's minimal essential medium were adsorbed onto VERO cell monolayers for 60 min at 37°C in 5% CO_2. After adsorption, the cells were overlaid with 3 ml of medium containing 3% fetal calf serum and 1% methyl cellulose. After 2 days of incubation (at 37°C) in a humidified atmosphere (5% CO_2), the cells were fixed with acetic acid and methanol (at a ratio of 1:3) and stained with crystal violet (1%). Plaques were counted in an inverted microscope.

Study protocol. These studies were carried out in conformance with the Position of the American Heart Association on Research Animal Use. A total of 239 mice form the basis of this study; the 30 day segment included 84 mice. Six mice were killed on day 0 (before infection); after infection, six were killed on day 10, five on day 20 and five on day 30. An additional five mice served as an age-matched uninfected control group for the 30 day segment and were never inoculated. Because of the high incidence of death from the disease, it was necessary to inoculate 150 mice (in batches of about 20) to obtain 6 that survived to the 150 day end point.

To exclude the possibility of prior infections, 9 to 11 week old inbred male C_3H/He mice (Jackson Laboratories) were isolated for 2 weeks before injection of virus and observed daily. At the age of 11 to 13 weeks, the mice were inoculated intraperitoneally with 10^3 plaque-forming units/0.1 ml of encephalomyocarditis virus. Twenty-eight mice were subjected to radionuclide ventriculography, antimyosin scan and biodistribution study at day 0 (before infection, n = 6) and at days 10 (n = 6), 20 (n = 5), 30 (n = 5) and 150 (n = 6) after infection. To monitor the serial ejection fraction values in naturally aging mice, the five uninfected control mice were subjected to ventriculography on days 0, 10 and 30. Immediately after the radionuclide ventriculographic studies had been completed, indium-111 antimyosin antibody imaging was performed at 24 and 48 h after injection; the preliminary data revealed that optimal target/background ratios were obtained at 48 h. The mice were then killed by bleeding from the retroorbital plexus at the stated time points and necropsied. At necropsy, the heart and other organs were processed for indium-111 antimyosin antibody biodistribution study, followed by histologic examination. Other mice that had died as a result of infection were also processed for virologic study.

Radionuclide ventriculography. After inoculation, radionuclide ventriculograms could be performed without anesthesia because mice were less active (in part due to paralysis of the limbs). Before inoculation and on day 150, the mice required anesthesia by intraperitoneal injection of sodium pentobarbital (8). The dose necessary to reach an anesthetic threshold was 0.045 and 0.060 mg/g of body weight (by the method of Pilgrim and De Ome [9]), a dose that does not affect cardiac physiology. The animals were placed in a supine position. Stannous pyrophosphate (0.1 to 0.15 mg/0.1 ml) was injected intravenously. Ten minutes later, 9 to 14 mCi/0.05 ml of technetium-99m pertechnetate was injected intravenously. The radionuclide ventriculogram was acquired by electrocardiographic (ECG) gating with a 2 mm pinhole collimator. Images were recorded in a 32×32 matrix in the anterior projection. The gamma camera (Elscint) was peaked to 140 keV with a 20% window. For each image, data were collected over 5 min (10). Because it is impossible in many mice to distinguish between the right and left ventricles (especially when the heart is dilated) on the radionuclide ventriculogram, we calculated a combined ejection fraction for both ventricles.

Because of the small aperture pinhole collimator and the need to shorten the imaging time, we administered a rather large dose of technetium-99m pertechnetate. This was necessary to prevent mice from dying from prolonged exposure to anesthesia and produce clear images.

Indium-111 antimyosin antibody cardiac scan. Monoclonal antibody 2G4 (a whole immunoglobulin G directed against the heavy chain of murine cardiac myosin) coupled to diethylene triamine pentaacetic acid for radiolabeling was used in this study. After the radiolabeled (130 μCi of indium-111 in 0.1 to 0.2 ml) pyrogen-free 2G4 (100 μg) had been administered intravenously, anterior static planar images (acquisition time of 10 min each) were obtained in a 256×256 matrix at 24 and 48 h (Elscint Apex Camera, 2 mm pinhole collimator). Both energy peaks (that is, 173 and 247 keV) were used with 10% windows.

Planar images were interpreted directly from the computer screen by at least three observers who had no knowledge of the pathologic findings. Antimyosin uptake was graded as follows: 0 = normal, 1+ = possible uptake, 2+ = definite but not intense uptake (< the sternal uptake), 3+ = definite, clear and intense uptake (= the sternal uptake), and 4+ = very intense uptake (≥ hepatic uptake). For a more objective evaluation, the heart/lung count density ratio was also calculated. After a region of interest was delineated in the anterior image over the heart and lower right lung, the mean count density (counts/pixel) in each area was determined and the heart/lung ratio calculated.

Biodistribution studies. These studies were performed to confirm antimyosin antibody 2G4 uptake by the heart and other organs by tissue counting and to characterize the distribution of the antibody. After the mice were killed,

indium-111 antimyosin distribution was measured in the blood, heart, lungs, liver, sternum, ribs, pancreas, spleen, kidneys, psoas muscle, skull and brain, and data were expressed as the percent of injected dose per gram of tissue (11). The biodistribution studies are an essential verification of the imaging studies.

Histopathology. Organs were fixed in 10% formalin solution and embedded in paraffin. Sections were made through the four chambers of the heart, stained with hematoxylin-eosin and examined in serial sections. Myocardial lesions, cellular infiltration, myocardial cell necrosis and fibrosis were scored in terms of severity by two blinded observers as follows: 0 = no lesions, 1+ = one or two small foci, 2+ = several small foci, 3+ = multiple small or several large foci and 4+ = multiple large foci.

Virus titers. For infectivity assays, the heart was removed, weighed and homogenized aseptically in 2 ml of Eagle's minimum essential medium. After centrifugation at 1,500 *g* for 15 min at 4°C, supernatant (0.1 ml) was inoculated into VERO cell monolayers and plaque assays were performed.

Statistics. Data were subjected to one- and two-way analysis of variance (with multiple sample comparisons) according to the Newman-Keul method (12). Correlations were calculated by simple regression analysis. Results were expressed as mean ± standard deviation.

Results

Mortality and incidence of myocarditis. Of the 84 mice in the 30 day segment of the study, a total of 17 were killed for data sampling before day 30. Of the remaining 67 mice, 25 infected mice (37%) died by day 10, 15 (22%) between days 11 and 20 and 22 (33%) between days 21 and 30; 5 mice survived for 30 days. The total cumulative mortality rate by day 30 was 92.5%. The incidence of myocarditis was 100%, both in the mice that were killed (confirmed by microscopic examination) and in those that died of infection (confirmed by macroscopic examination).

Radionuclide ventriculography (Table 1, Fig. 1). The baseline ejection fraction in the uninfected mice (day 0) was 63.3 ± 3.1%. Infected mice showed a lower ejection fraction on days 10 (20.7 ± 5.5%), 20 (18.6 ± 15.2%), 30 (18.5 ± 7.7%) and 150 (30.0 ± 18.7%) in comparison with that in control mice ($p < 0.001$ in each group). Ejection fraction for the five age-matched control mice that had not been infected was constant and within normal range throughout the course of the study. The difference in ejection fraction between the infected group and the uninfected age-matched group was significant on days 10 and 30 ($p < 0.001$).

Antimyosin scan (Table 1, Fig. 2). None of the uninfected mice on day 0 (baseline) showed myocardial uptake (score of 0). On day 10, dense antimyosin uptake was seen in the myocardium of all six mice (score of 2.5 ± 0.6). On day 20, however, small and focal uptake was seen in only one of five mice (score of 1). On days 30 and 150, only two mice had a positive score (score of 2 and 1, and 1.5 and 0.5, respectively). The heart/lung ratio of the mean count density in the region of interest drawn around the heart and lungs is also shown in Table 1. There was a good correlation ($p < 0.0001$) between the scores by subjective grading of antimyosin scan and the calculations of heart/lung ratio.

Biodistribution of indium-111 antimyosin antibody and myocardium to blood ratios (Table 2). Uptake in the myocardium was measured in the whole heart. The heart to blood uptake ratio on day 10 was high ($p < 0.001$ versus that in the mice before infection), but not on days 20, 30 and 150. As already described (Table 1), myocardial uptake grade and heart/lung count density ratio correlated well.

Pathologic findings (Table 1, Fig. 3). Serial pathologic studies in this model have been described elsewhere (7,8). In brief, by days 3 to 4, the mice appeared irritable and ill (with coat ruffling). Paralysis of the lower limbs first appeared on day 5, when yellow-white patches could be seen macroscopically on the surface of the heart. On day 10, paralysis of the lower limbs was fixed. At this stage, marked cellular infiltration and myocardial necrosis were evident microscopically (Fig. 3). On day 20, cellular infiltration and myocardial necrosis decreased, and the process of healing (that is, evidence of fibrosis) commenced. Pleural effusion and ascites were found on days 10 through 30, and pulmonary and hepatic congestion was evident microscopically. With the exception of the brain and pancreas, neither inflammatory nor necrotic lesions were noted in other organs. No abnormalities were found in organs from the uninfected mice.

Virologic study. Encephalomyocarditis virus was isolated from the hearts of mice on days 8 and 9 ($14.17 \pm 5.17 \times 10^6$ plaque-forming units/g tissue, n = 9) and on days 10 and 11 ($7.19 \pm 7.75 \times 10^4$ plaque-forming units/g tissue, n = 10). No virus was isolated on days 15 through 21 (n = 5).

Discussion

Murine viral myocarditis. The evolution of cardiac histopathology in this model of viral myocarditis is in agreement with our previous studies (7,8). Infiltration and necrosis were most severe at 10 days after infection; infiltration was absent at 150 days (except in one of six mice), although focal necrosis was still visible; fibrosis appeared as early as day 10 and progressed until day 20, but stabilized thereafter.

Although murine myocarditis induced by infection with a cardiotropic strain of the encephalomyocarditis virus has been studied extensively (7,8), ours is the first study of global cardiac systolic function in the mouse model. Against a background of reasonably reproducible and constant values in control mice, the present study indicates a significant, substantial and consistent decrease in systolic function at 10, 20 and 30 days after infection and a partial recovery 150 days after infection. This pattern of change in systolic function correlates well with the degree of cellular infiltration and myocardial necrosis.

Table 1. Radionuclide Ejection Fraction, Antimyosin Scan Grade (uptake in heart), Heart/Lung Mean Count Density Ratio for Antimyosin Scan and Histopathologic Grade of Myocarditis

	Days				
Mouse No.	0 (n = 6)	10 (n = 6)	20 (n = 5)	30 (n = 5)	150 (n = 6)
EF (%)*					
1	60	25	6	12	7
2	64	22	14	23	9
3	62	14	12	27	40
4	69	15	45	—†	45
5	62	20	16	12	28
6	63	28			51
	63.3 ± 3.1	20.7 ± 5.5‡	18.6 ± 15.2‡	18.5 ± 7.7‡	30.0 ± 18.7‡
Antimyosin scan (uptake 0 to 4+)					
1	0	3.5	—§	2.0‖	0
2	0	3.0	0	1.0	1.5
3	0	2.5	1.0	0	0
4	0	2.0	0	—†	0
5	0	2.0	0	0	0.5
6	0	2.0			0
	0 ± 0	2.5 ± 0.6‡	0.3 ± 0.5	0.8 ± 1.0	0.3 ± 0.6
Antimyosin scan heart/lung ratio (mean count density ratio)					
1	1.42	5.22	—§	2.15‖	0.83
2	1.07	3.67	0.86	1.14	1.57
3	1.15	2.75	1.09	1.38	1.15
4	0.80	2.94	0.89	—†	0.92
5	1.09	2.35	1.00	1.04	1.45
6	1.28	1.92			0.93
	1.14 ± 0.21	3.14 ± 1.17‡	0.96 ± 0.11	1.43 ± 0.50	1.14 ± 0.31
Infiltration					
1	0	3	3	2	0
2	0	3	3	1	1
3	0	3	2	1	0
4	0	3	1	2	0
5	0	4	2	1	0
6	0	4			0
	0 ± 0	3.3 ± 0.5‡	2.2 ± 0.8‡	1.4 ± 0.5‡	0.2 ± 0.4
Pathologic grade (0 to 4+) Necrosis					
1	0	4	3	3	1
2	0	4	3	2	2
3	0	4	3	2	1
4	0	4	3	2	1
5	0	4	4	4	2
6	0	4			2
	0 ± 0	4.0 ± 0.0‡	3.2 ± 0.4‡	2.6 ± 0.9‡	1.5 ± 0.5‡
Fibrosis					
1	0	1	3	2	2
2	0	1	2	3	2
3	0	1	2	2	2
4	0	1	2	2	2
5	0	2	2	3	3
6	0	2			1
	0 ± 0	1.3 ± 0.5‡	2.2 ± 0.4‡	2.4 ± 0.5‡	2.0 ± 0.6‡

*Ejection fraction (EF) was evaluated in a group of five uninfected mice (data not shown) on days 0, 10 and 30 and was found to be almost constant: day 0 = 59.2 ± 5.7%; day 10 = 53.2 ± 2.2%; day 30 = 56.8 ± 11.2%. †This mouse died of rhythm disturbance during radionuclide ventriculography. ‡$p < 0.001$ versus values on day 0. §This mouse died 24 h after radionuclide ventriculography but before antimyosin scan. ‖This mouse died 24 h after antimyosin scan. Values are mean ± SD.

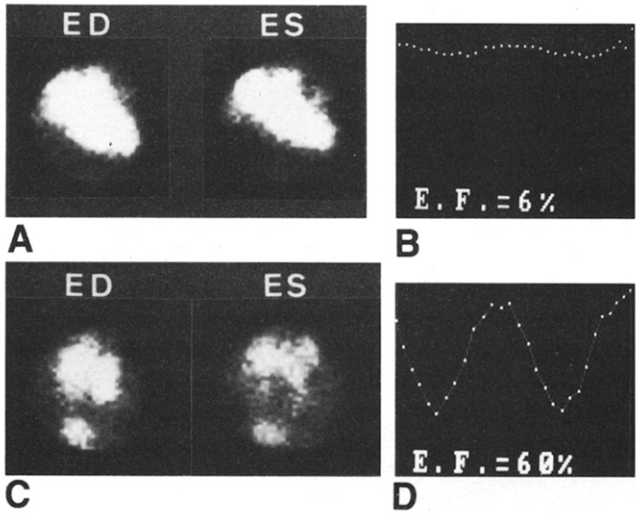

Figure 1. Radionuclide ventriculograms and time-activity curves in diseased (**A** and **B**) and uninfected (**C** and **D**) mice. Ejection fraction (E.F.) in an infected mouse on day 10 (6%, **A** and **B**) was apparently low compared with that in a control mouse (60%, **C** and **D**). Also note that the separation of the left and right ventricles was not clear in the enlarged diseased heart. However, in the control mouse, the right and left ventricles are separated by the septum. ED = end-diastole; ES = end-systole.

Antimyosin antibody scans to diagnose acute myocarditis. Radiolabeled immunoglobulin G antibodies to myosin bind cells that have lost the integrity of their plasma membranes: when the membrane degenerates, intracellular myosin is exposed to extracellular fluid. Scintigraphic examinations with these antibodies have been used to localize and quantify regions of myocardial necrosis in myocardial infarction (13–17). In a clinical study of antimyosin antibody scans in a series of 28 patients suspected of having myocarditis, Yasuda et al. (5) reported a sensitivity of 100% but a specificity of only 58%. Most recently, Matsumori et al. (18) studied the myocardial uptake of iodine-125– and iodine-131–labeled monoclonal antimyosin Fab in experimental murine viral encephalomyocarditis over a period of 28 days. They (18) showed that antimyosin Fab localized selectively in hearts

Figure 2. Antimyosin antibody scan. Note the dense myocardial uptake (**arrow**) in a diseased mouse on day 10 (**A**) and the normal uptake in a control mouse (**B**).

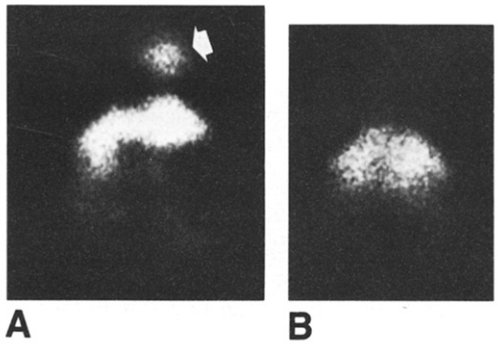

Table 2. Biodistribution of Indium-111-Labeled Antimyosin Antibody in Tissues of Mice Before and After Infection With Virus

Mice	Blood	Heart	Lung	Liver	Spleen	Pancreas	Kidney	Rib	Sternum	Muscle	Brain	Heart/Blood Ratio
Before infection (n = 6)	0.38 ± 0.04	0.34 ± 0.07	0.36 ± 0.04	1.09 ± 0.11	0.39 ± 0.08	0.22 ± 0.04	1.26 ± 0.10	0.17 ± 0.04	0.19 ± 0.03	0.08 ± 0.01	0.01 ± 0.01	0.88 ± 0.11
After infection												
Day 10 (n = 5*)	0.45 ± 0.03	1.54 ± 0.75	0.60 ± 0.18	3.04 ± 1.16	0.53 ± 0.17	0.24 ± 0.04	1.28 ± 0.29	0.26 ± 0.10	0.30 ± 0.05	0.17 ± 0.12	0.02 ± 0.01	3.43 ± 1.56
p value	NS	<0.001	NS	<0.05	NS	NS	NS	NS	NS	NS	<0.05	<0.001
Day 20 (n = 4)	0.34 ± 0.10	0.61 ± 0.23	0.96 ± 0.61	3.23 ± 1.82	0.75 ± 0.14	0.22 ± 0.07	3.68 ± 1.05	0.71 ± 0.74	0.58 ± 0.39	0.26 ± 0.13	0.03 ± 0.01	1.94 ± 0.85
p value	NS	NS	<0.01	<0.05	<0.05	NS	<0.001	NS	<0.01	NS	<0.001	NS
Day 30 (n = 3)	0.31 ± 0.01	0.30 ± 0.02	0.30 ± 0.03	1.57 ± 0.26	0.52 ± 0.07	0.12 ± 0.05	1.33 ± 0.09	0.24 ± 0.14	0.22 ± 0.06	0.08 ± 0.01	0.01 ± 0.00	0.99 ± 0.05
p value	NS	NS	NS	NS	NS	NS	NS	NS	NS	NS	NS	NS
Day 150 (n = 6)	0.40 ± 0.09	0.36 ± 0.10	0.32 ± 0.09	1.70 ± 0.10	0.58 ± 0.21	0.23 ± 0.09	1.43 ± 0.23	0.17 ± 0.05	0.21 ± 0.13	0.14 ± 0.13	0.02 ± 0.01	0.88 ± 0.10
p value	NS	NS	NS	NS	NS	NS	NS	NS	NS	NS	NS	NS

*One mouse was excluded because of infiltrated injection. p values denote the results of comparison with uninfected mice. Results are expressed as % injected dose/g tissue weight. Values are mean ± SD.

Figure 3. Cardiac histopathologic specimen from an infected mouse on day 10 (same mouse as in Fig. 2A). Prominent cellular infiltration with active myocardial necrosis is evident. Hematoxylin-eosin stain ×500, reduced by 31%.

from the acute and subacute stages of the disease. Because myocardial necrosis is an essential manifestation of the disease process, the present study confirms the applicability of radiolabeled antimyosin imaging in the diagnosis of myocarditis. Indeed, the results of the biodistribution studies confirm that there is an abnormal accumulation of indium-111 antimyosin antibody in diseased hearts. The data also demonstrate that a negative antimyosin scan reflects either the absence of or the healing stage of myocarditis. Therefore in the clinical setting, a negative antimyosin scan probably excludes the presence of myocarditis in the acute phase.

Correlation with histopathologic findings. Myocardial uptake of antimyosin antibody, as revealed by in vivo scanning, was strongly positive at 10 days after infection, a time at which histopathologic evidence of necrosis was also maximal. Thereafter, uptake was sporadic and weak. In agreement with these results, in vitro uptake of indium-111 in heart tissue was significant only on day 10. Our hypothesis is that in the early stage of myocardial necrosis, there is an abundant supply of myosin binding sites still in possession of a molecular structure recognizable by antimyosin antibodies. With the passage of time the structure probably loses its specificity for the antibodies and binding to necrotic areas decreases. This would explain the discrepancy after day 10 between the degree of necrosis by pathologic criteria and that by antimyosin antibody uptake. In any case, the results of this study fulfill expectations about antimyosin antibody uptake: uptake correlates well with evidence of acute myocardial necrosis by histopathology and with evidence of systolic dysfunction.

Systolic function in myocarditis. Previous studies (7,8,19) of viral encephalomyocarditis provide evidence of depressed cardiac function by several indirect criteria (namely, cardiac pathology, congestion of the lungs and liver and low voltage QRS complexes with tachycardia on the ECG). In the present study, we measured ejection fraction directly by ECG-gated ventriculography. The marked decrease in ejection fraction in the acute and subacute stages of myocarditis and the partial recovery of ejection fraction in the chronic stage parallel what has been observed in clinical settings. The depression of global cardiac function in the acute stage is associated with severe myocardial damage and intense myocardial uptake of antimyosin. Mice that survived the acute stage tended to show less myocardial necrosis and less uptake of antimyosin in the myocardium; indeed, the ejection fraction in mice on day 150 was higher than that on day 10. This could reflect the survival or recovery of mice least affected by the disease.

It is of interest that even in the chronic stage, some mice (two of five on day 30 and two of six on day 150) showed positive antimyosin uptake associated with a low ejection fraction, which suggests active and ongoing myocardial necrosis. Even after careful evaluation of cardiac pathology (light microscopy of hematoxylin-eosin stained samples), no definitive evidence of the active process of myocardial necrosis could be found. It must be recognized, however, that notwithstanding the genetic homogeneity and uniform sensitivity of the mice to the virus, the survivors were heterogeneous in cardiac function and pathology.

Clinical implications. Although this experimental study involves a single virus (not pathogenic to humans), one inbred strain of mice and a known time of infection as opposed to clinical studies that involve multiple viruses (or other causes of myocardial damage), an outbred species and unknown duration of disease, a valid comparison can be made between the time course of myocarditis in these two settings. The period of 10 days after infection in the murine model would be comparable with the onset of clinical

symptoms (the appearance of chest pain, ECG abnormalities and other cardiac manifestations of disease) (19,20). The 20 day period would mirror the stage of definitive clinical manifestations of myocarditis and severe cardiac dysfunction. Thus, antimyosin antibody imaging may be the first noninvasive method for the detection of necrotic processes underlying even the chronic stage of myocarditis, during which unknown or immune mechanisms may be in operation (8,20,21). In the setting of increasing evidence of the lack of sensitivity of endomyocardial biopsy for the detection of active myocarditis in humans the results of this experimental study support the conclusions of our pilot clinical study (5) and justify further evaluation of antimyosin scanning in the diagnosis of myocarditis.

We thank Kathryn A. Thorp for technical help, Joan Burke and Tom McVarish for assistance in preparing the manuscript and Rosemary Kennedy for support in carrying out this project.

References

1. Aretz HT, Billingham ME, Edwards WD, et al. Myocarditis: a histopathologic definition and classification. Am J Cardiovasc Pathol 1986;1: 3–14.
2. Dec GW Jr, Palacios IF, Fallon JT, et al. Active myocarditis in the spectrum of acute dilated cardiomyopathies: clinical features, histologic correlates, and clinical outcome. N Engl J Med 1985;312:885–9.
3. Abelmann WH. Viral myocarditis and its sequelae. Annu Rev Med 1973;24:145–52.
4. Kawai C. Idiopathic cardiomyopathy: a study on the infectious-immune theory as a cause of the disease. Jpn Circ J 1971;35:765–8.
5. Yasuda T, Palacios IF, Dec GW, et al. Indium-111 monoclonal antimyosin antibody imaging in the diagnosis of acute myocarditis. Circulation 1987;76:306–11.
6. Carrio I, Berna L, Ballester M, et al. Indium-111 antimyosin scintigraphy to assess myocardial damage in patients with suspected myocarditis and cardiac rejection. J Nucl Med 1988;29:1893–900.
7. Kishimoto C, Kuribayashi K, Masuda T, Tomioka N, Kawai C. Immunological behavior of lymphocytes in experimental viral myocarditis: significance of T lymphocytes in the severity of myocarditis and silent myocarditis in BALB/c-nu/nu mice. Circulation 1985;71:1247–54.
8. Kishimoto C, Kuribayashi K, Fukuma K, et al. Immunologic identification of lymphocyte subsets in experimental murine myocarditis with encephalomyocarditis virus: different kinetics of lymphocyte subsets between the heart and the peripheral blood, and significance of Thy 1.2^+ (pan T) and Lyt 1^+, 23^+ (immature T) subsets in the development of myocarditis. Circ Res 1987;61:715–25.
9. Pilgrim HI, De Ome KE. Intraperitoneal pentobarbital anesthesia in mice. Exp Med Surg 1955;13:401–3.
10. Strauss HW, Zaret BL, Hurley PJ, Natarajan TK, Pitt B. A scintiphotographic method for measuring left ventricular ejection fraction in man without cardiac catheterization. Am J Cardiol 1971;28:575–80.
11. Chase GD, Rabinowitz JL. Principles of Radioisotope Methodology. 3rd ed. Minneapolis: Burgess, 1967:465–8.
12. Zar JH. Biostatistical Analysis. Princeton, NJ: Prentice-Hall, 1974;151–5.
13. Khaw BA, Fallon JT, Beller GA, Haber E. Specificity of localization of myosin-specific antibody fragments in experimental myocardial infarction: histologic, histochemical, autoradiographic and scintigraphic studies. Circulation 1979;60:1527–631.
14. Khaw B, Beller GA, Haber E, Smith TW. Localization of cardiac myosin-specific antibody in myocardial infarction. J Clin Invest 1976;58: 439–46.
15. Khaw BA, Gold HK, Leinbach RC, et al. Early imaging of experimental myocardial infarction by intracoronary administration of ^{131}I-labeled anticardiac myosin $(Fab')_2$ fragments. Circulation 1978;58:1137–42.
16. Khaw BA, Fallon JT, Strauss HW, Haber E. Myocardial infarct imaging of antibodies to canine cardiac myosin with indium-111-diethylenetriamine pentaacetic acid. Science 1980;209:295–7.
17. Khaw BA, Gold HK, Yasuda T, et al. Scintigraphic quantification of myocardial necrosis in patients after intravenous injection of myosin-specific antibody. Circulation 1976;74:501–8.
18. Matsumori A, Ohkusa T, Matoba Y, et al. Myocardial uptake of antimyosin monoclonal antibody in a murine model of viral myocarditis. Circulation 1989;79:400–5.
19. Kishimoto C, Matsumori A, Ohmae M, Tomioka N, Kawai C. Electrocardiographic findings in experimental myocarditis in DBA/2 mice: complete atrioventricular block in the acute stage, low voltage of the QRS complex in the subacute stage and arrhythmias in the chronic stage. J Am Coll Cardiol 1984;3:1461–8.
20. Woodruff JF. Viral myocarditis: a review. Am J Pathol 1980;101:427–84.
21. Kishimoto C, Misaki T, Crumpacker CS, Abelmann WH. Serial immunologic identification of lymphocyte subsets in murine coxsackievirus B3 myocarditis: different kinetics and significance of lymphocyte subsets in the heart and in peripheral blood. Circulation 1988;77:645–53.